[Supporting Information]

Tunable Photocatalytic Water Splitting and Solar-to-Hydrogen Efficiency in β-PdSe₂ Monolayer

Mukesh Jakhar and Ashok Kumar*

Department of Physics, School of Basic Sciences, Central University of Punjab, Bathinda, 151401, India

(August 13, 2021)

*Email:

ashokphy@cup.edu.in (Ashok Kumar)

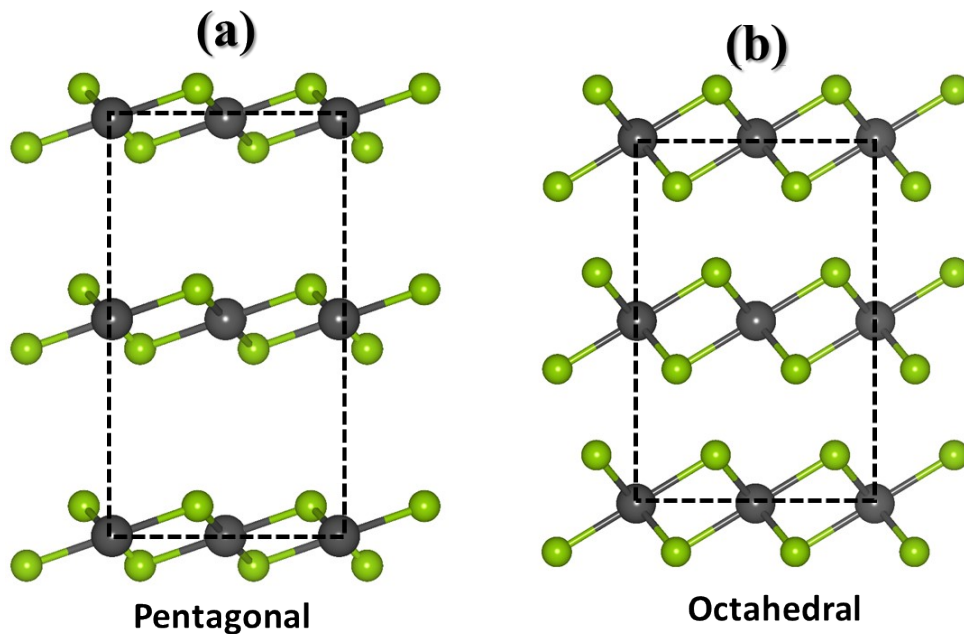# 1. Crystal structure and lattice parameters of bulk Penta- PdSe$_2$, Octa- PdSe$_2$ and β- PdSe$_2$

Fig. S1 Crystal structure of bulk (a) Pentagonal PdSe$_2$ (b) Octahedral PdSe$_2$.

Table S1. The calculated lattice parameters for bulk Pentagonal, Octahedral, β-PdSe$_2$, and β-PdSe$_2$ monolayer respectively.

Structures	Lattice constants			Cohesive Energy (eV/atom)	Reference
	a (Å)	b (Å)	c (Å)		
Bulk Penta- PdSe$_2$	5.63 (5.74)[1]	5.89 (5.86)[1]	7.57 (7.69)[1]	5.60	**This Work** (Ref)[1]
Bulk Octa- PdSe$_2$	3.77 (3.80)[2]	3.77 (3.80)[2]	4.98 (4.91)[2]	5.94	**This Work** (Ref)[2]
Bulk β- PdSe$_2$	3.65	4.35	4.38	5.69	**This Work**
Monolayer β- PdSe$_2$	3.60	4.36	-	5.54	**This Work**

2. The AIMD energy fluctuations at 500 K and 1000K for β- PdSe$_2$ monolayer.
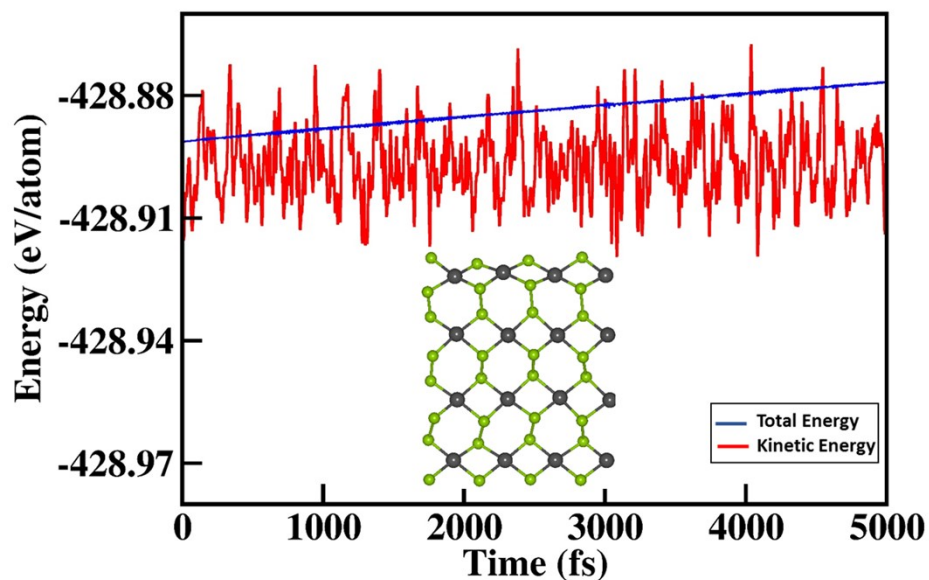

Fig. S2 The AIMD kinetic and total energy fluctuations at 500 K, and the snapshot of the equilibrium structure (in insets) after 5000 fs for β-PdSe$_2$ monolayer.
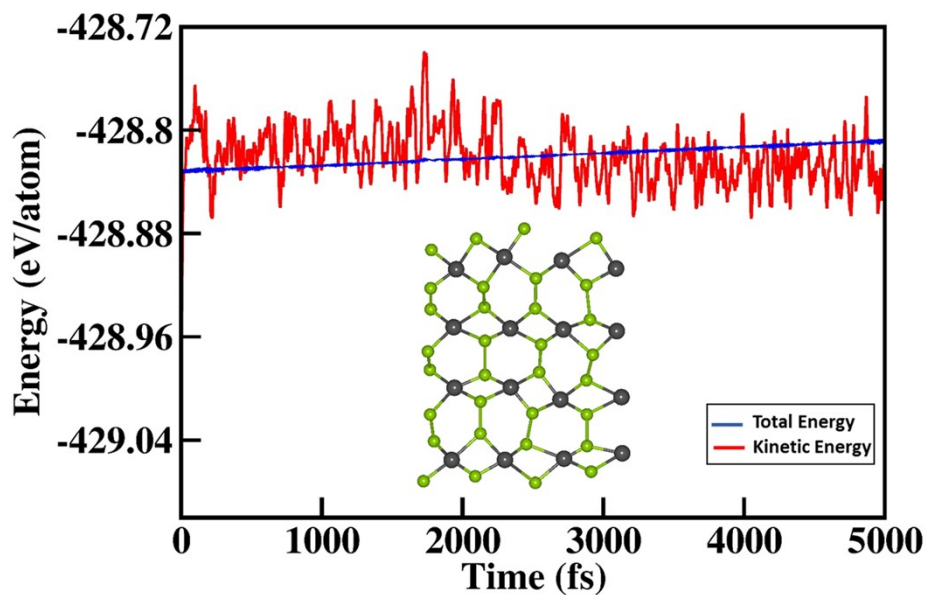

Fig. S3 The AIMD kinetic and total energy fluctuations at 1000 K, and the snapshot of the equilibrium structure (in insets) after 5000 fs for β-PdSe$_2$ monolayer.

3. Electronic band structure for bulk β-PdSe₂ and β-PdSe2 monolayer with spin-orbital coupling (SOC) extracted from PBE functional.
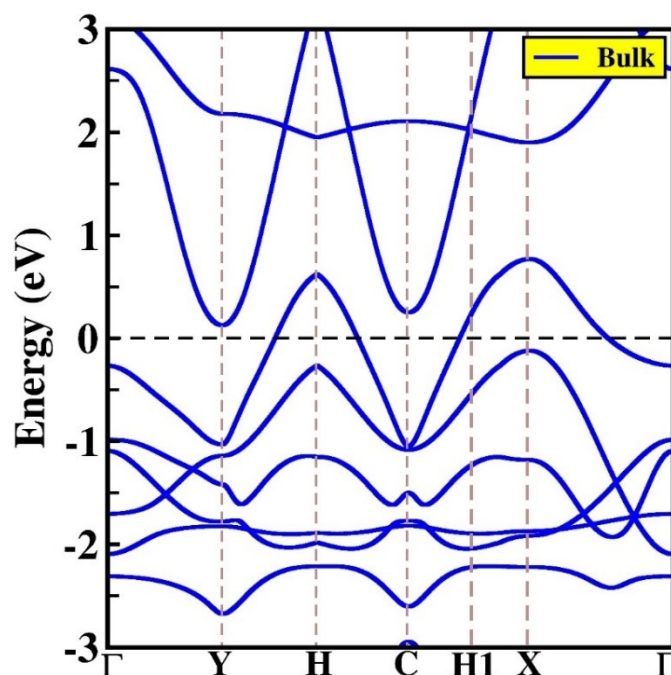

Fig. S4 The calculated electronic band structure of β-PdSe$_2$ bulk extracted from PBE functional.
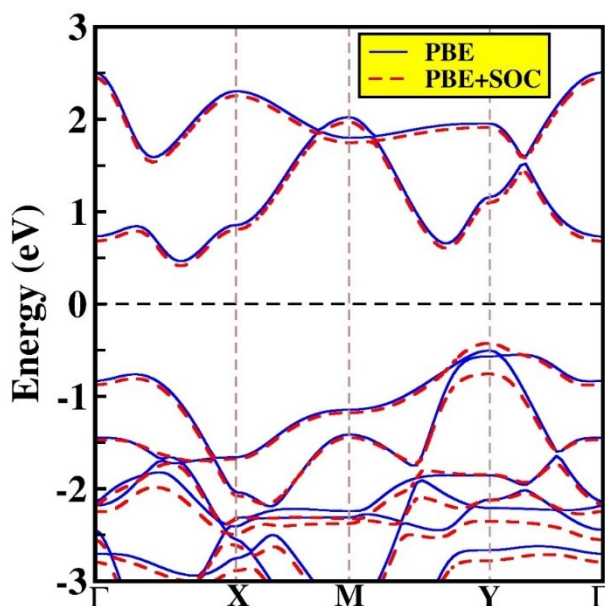

Fig. S5 The calculated electronic band structure of β-PdSe$_2$ monolayer with spin-orbital coupling (SOC) (red), and without SOC (blue) extracted from PBE functional.

4. Charge carrier mobility for β-PdSe₂ monolayer.

The charge carrier mobilities have been calculated using $\mu_{2D} = \dfrac{e\hbar^3 C_{2D}}{K_B T m^* m_a^* E_i^2}$ where, C_{2D} is the elastic modulus of the material along transport direction and is given by $C_{2D} = \dfrac{1}{S_0}\left(\dfrac{\delta^2 E_{total}}{\delta\epsilon^2}\right)$.

E_{total}, ϵ, and S_0 are the total energy, uniaxial strain, and area of the unstrained unit cell, respectively. E_i is the deformation potential which is defined as $E_i \dfrac{\delta E_{edge}}{\delta\epsilon}$, where E_{edge} is the energy of VBM or CBM. m^* is the effective mass in the transport direction (i.e., either along x or y direction), and m_a^* is the average effective mass given by $\sqrt{m_x^* m_y^*}$.

Table S2: β-PdSe₂ monolayer: The effective mass (m^*), the elastic modulus of the material (C_{2D}), the deformation potential (E_i), and the charge carrier mobilities (μ_{2D}).

Material	Charge Type	m^*/m_0	C_{2D} (J/m²)	E_i (eV)	$\mu_{2D}(cm^2V^{-1}s^{-1})$
	$h(x)$	1.22	59.64	-3.80	70.36
	$e(x)$	0.96	59.64	0.64	4559.08
β -PdSe₂	$h(y)$	0.92	15.59	-2.88	42.47
	$e(y)$	0.72	15.59	-4.48	32.63

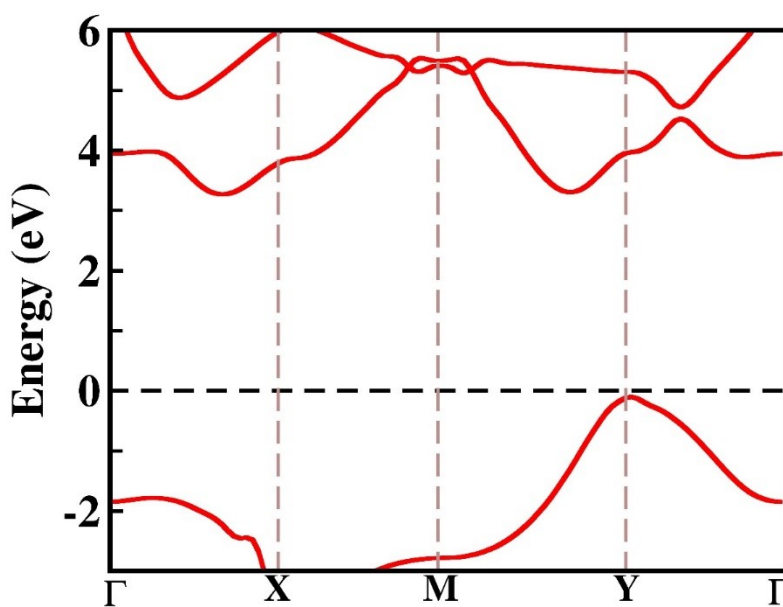# 5. Electronic band structure for β-PdSe2 monolayer extracted from GW corrections.

Fig. S6 The calculated electronic band structure of β-PdSe$_2$ monolayer extracted from GW corrections.

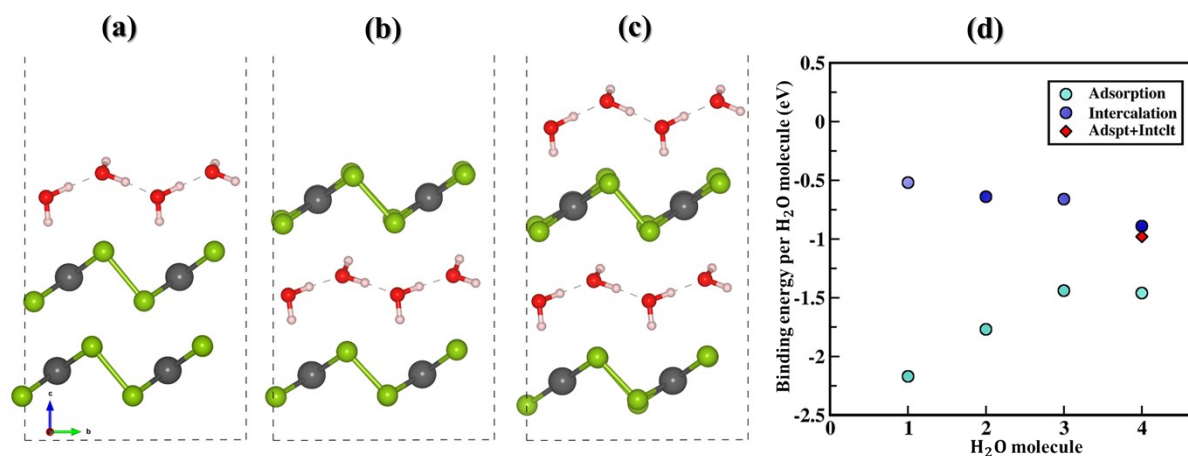# 5. Adsorption/Intercalation Energies on (001) surface of β-PdSe$_2$ monolayer.

Fig. S7 (a) Adsorption model (b) intercalation model with 4 H$_2$O molecules on (001) surface of β-PdSe$_2$ (c) Adsorption + intercalation model with 4 H$_2$O molecules intercalated in layers and 4 H$_2$O molecules on (001) surface of β-PdSe$_2$. (d) Binding energies of adsorption and intercalation models for (001) surface of β-PdSe$_2$.

6. Hydrogen evolution reaction (HER) as a function of hydrogen coverage on β-PdSe₂ monolayer.
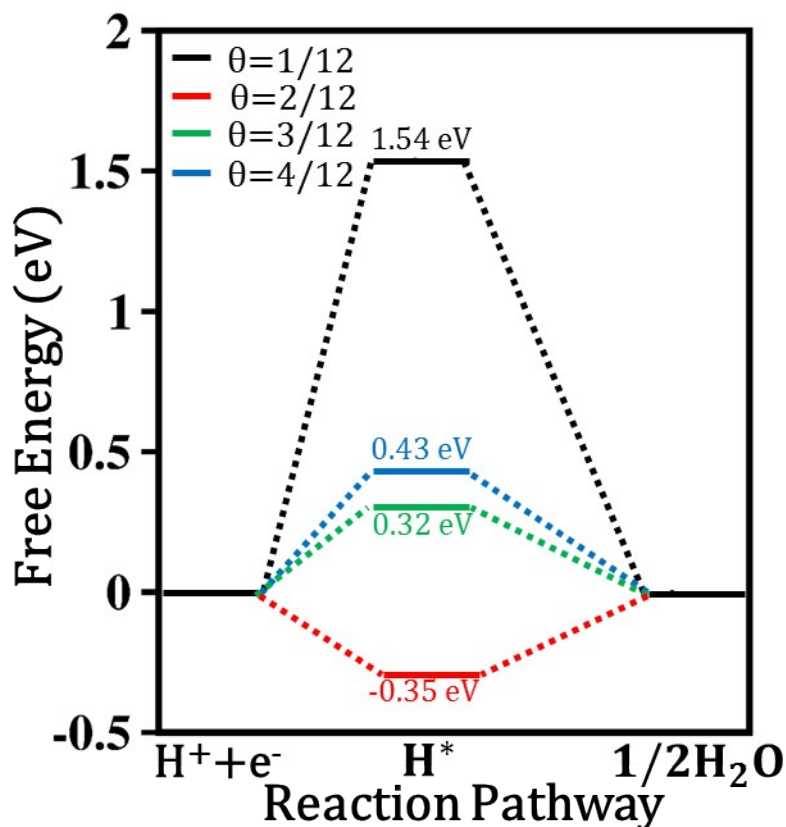
Fig. S8 Free energy reaction steps of HER as a function of hydrogen coverage on β-PdSe₂ monolayer.

Table S3. The calculated total energy (E*) of catalysts, the adsorption energy of H∗ intermediates (E$_{H∗}$), and the difference free energy of hydrogen adsorption (ΔG$_{H∗}$) with different hydrogen coverage on β -PdSe₂ monolayer.

Species	E* (eV)	Concentration	E$_{H∗}$ (eV)	ΔG$_{H∗}$ (eV)
		1/12	-5173.847021	1.54
β-PdSe₂	-5159.643214	2/12	-5189.951060	-0.35

		3/12	-5205.378831	0.32
		4/12	-5220.784349	0.43

7. Computational details of free energy change (ΔG) for β-PdSe₂ monolayer.

The OER is highly pH-sensitive; the acidic mechanism involves the production of $H^+ + e^-$ pairs, and their Gibbs free energy is usually calculated implicitly by assuming the equilibrium $H^+ + e^- \leftrightarrow 1/2H_2$ at standard conditions (pH = 0, pressure pH_2 = 1 bar, and T = 298.15 K), while alkaline mechanism involves the oxidation of OH^- with concomitant release of e^-.

OER using an acidic reaction mechanism

Here we consider a four-electron reaction mechanism for acidic medium,

$$H_2O\ (1) + \ * \rightleftharpoons \ *OH + H^+ + e^- \tag{1}$$

$$*OH \rightleftharpoons \ *O + H^+ + e^- \tag{2}$$

$$H_2O\ (1) + *O \rightleftharpoons \ *OOH + H^+ + e^- \tag{3}$$

$$*OOH \rightleftharpoons \ *+ O_2(g) + H^+ + e^- \tag{4}$$

where $*$ represents the active site of the catalyst, (g) refers to the gas phase, and $*OH$, $*O$, and $*OOH$ represents the species adsorbed on the active site as mentioned in Figure 6(c).

The typical procedure widely used in the literature to calculate the reaction Gibbs free energies, ΔG_n corresponding to equations (1)–(4) at standard conditions, is shown in equations (5)–(8);

$$\Delta G_1 = G(\ *OH) + G(H^+ + e^-) - G(\ *) - G(H_2O) - eU_{SHE} \tag{5}$$

$$\Delta G_2 = G(\ *O) + G(H^+ + e^-) - G(\ *OH) - eU_{SHE} \tag{6}$$

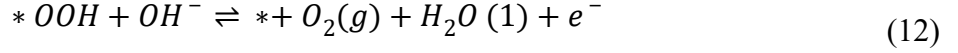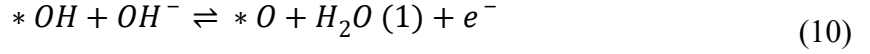$$\Delta G_3 = G(\ *OOH) + G(H^+ + e^-) - G(\ *O) - 2G(H_2O) - eU_{SHE} \tag{7}$$

$$\Delta G_4 = 4.92\ [eV] + [G(\ *) + 2G(H_2O)] - [G(\ *OOH) + 3G(H^+ + e^-)] - [eU_{SHE}] \tag{8}$$

eU_{SHE} is the potential of the electrode relative to the (standard hydrogen electrode) SHE.

OER using an alkaline reaction mechanism

This reaction is usually assumed to proceed in four elementary steps[3]

$$*+ OH^- \rightleftharpoons *OH + e^- \tag{9}$$

$$*OH + OH^- \rightleftharpoons *O + H_2O \,(1) + e^- \tag{10}$$

$$*O + OH^- \rightleftharpoons *OOH + e^- \tag{11}$$

$$*OOH + OH^- \rightleftharpoons *+ O_2(g) + H_2O\,(1) + e^- \tag{12}$$

The final expressions for the reaction Gibbs free energies using an alkaline reaction mechanism become

$$\Delta G_1 = G(*OH) + G(H^+ + e^-) - G(*) - G(H_2O) - eU_{RHE} \tag{13}$$

$$\Delta G_2 = G(*O) + G(H^+ + e^-) - G(*OH) - eU_{RHE} \tag{14}$$

$$\Delta G_3 = G(*OOH) + G(H^+ + e^-) - G(*O) - 2G(H_2O) - eU_{RHE} \tag{15}$$

$$\Delta G_4 = 4.92\,[eV] + \left[G(*) + 2G(H_2O)\right] - \left[G(*OOH) + 3G(H^+ + e^-)\right] - [eU_{RHE}] \tag{16}$$

eU_{RHE} is the potential of the electrode relative to the reversible hydrogen electrode (RHE) The electrode potential of the two reference potentials can be linked according to[4]

$$eU_{RHE} = eU_{SHE} - k_B T \ln a_{H^+} = eU_{SHE} + k_B T \times pH \times \ln 10 = \Delta G_U \tag{17}$$

where a_{H^+} is the activity of the H$^+$ ions in solution and at T = 298.15 K one has

$$k_B T \times pH \times \ln 10 = 0.059 \times pH = \Delta G_{pH} \tag{18}$$

Substituting equation (17-18) into equations (13)–(16) Then, considering the effect of electrode potential (U) and pH, the free energy change for OER electrochemical steps can be expressed as:

$$\Delta G_1 = G(*OH) + G(H^+ + e^-) - G(*) - G(H_2O) - \Delta G_U - \Delta G_{pH} \tag{19}$$

$$\Delta G_2 = G(*O) + G(H^+ + e^-) - G(*OH) - \Delta G_U - \Delta G_{pH} \tag{20}$$

$$\Delta G_3 = G(*OOH) + G(H^+ + e^-) - G(*O) - 2G(H_2O) - \Delta G_U - \Delta G_{pH} \tag{21}$$

$$\Delta G_4 = 4.92\,[eV] + \left[G(*) + 2G(H_2O)\right] - \left[G(*OOH) + 3G(H^+ + e^-)\right] - [\Delta G_U + \Delta G_{pH}] \tag{22}$$

The equations (19)–(22) can be used for calculating the reaction Gibbs free energies and the overpotential for the OER at all pH values for both acidic and alkaline mechanisms.

Table S4. Zero-pint energy correction (E$_{ZPE}$), entropy contribution (TS, T=298.15K), total energy (E), and the Gibbs free energy (G) of molecules and adsorbents on β -PdSe$_2$ monolayer.

Adsorbents	E_{ZPE} (eV)	$-TS$ (eV)	E (eV)	G (eV)
H_2	0.31	-0.41	-31.289192	-31.382345
H_2O	0.61	-0.67	-478.299089	-478.361973
*	-	-	-5159.643214	-5159.643214
*O	0.06	-0.00	-5603.833913	-5603.76
*OH	0.33	-0.00	-5620.640875	-5620.3157
*OOH	0.42	-0.21	-6065.156270	-6064.94627
*H	0.058	-0.00	-5173.847021	-5173.78881

8. Solar-to-Hydrogen (STH) Efficiency

η_{STH} is estimated by $\eta_{STH} = \eta_{abs} \times \eta_{cu}$ where η_{abs} is the efficiency of light absorption and η_{cu} is carrier utilization. The efficiency of carrier utilization as (η_{cu}) is defined as

$$\eta_{cu} = \frac{\Delta G \int_{E}^{\infty} \frac{P(\hbar\omega)}{\hbar\omega} d(\hbar\omega)}{\int_{E_g}^{\infty} P(\hbar\omega) d(\hbar\omega)}$$

(23)

Where ΔG is the potential difference for water splitting (1.23 eV) and E is the energy of photons that can be used for water splitting, which is determined by

$$E = \begin{cases} E_g, \left(\chi(H_2) \geq 0.2, \chi(O_2) \geq 0.6\right) \\ E_g + 0.2 - \chi(H_2), \left(\chi(H_2) < 0.2, \chi(O_2) \geq 0.6\right) \\ E_g + 0.6 - \chi(O_2), \left(\chi(H_2) \geq 0.2, \chi(O_2) < 0.6\right) \\ E_g + 0.8 - \chi(H_2) - \chi(O_2), \left(\chi(H_2) < 0.2, \chi(O_2) < 0.6\right) \end{cases}$$

Where, $\chi(H_2)$ is over potential for HER, and $\chi(O_2)$ is over the potential for oxygen evolution reaction (OER). Considering the previous reports of experiments and theoretical calculations, the required over potentials for HER and OER are assumed to be 0.2 and 0.6 eV, respectively[5, 6].
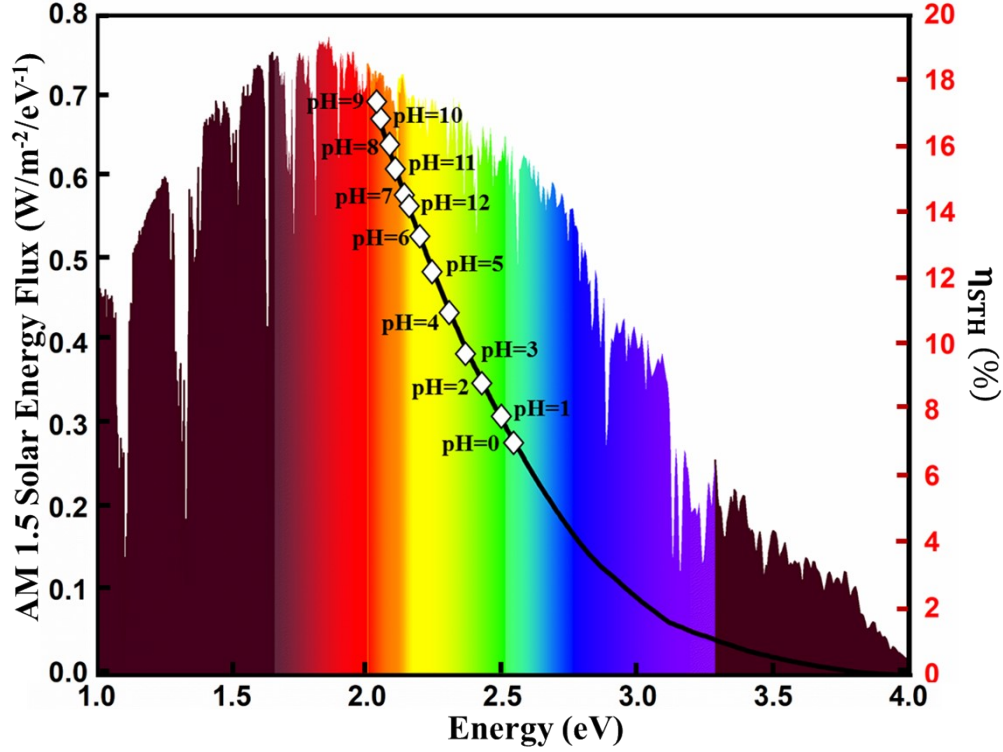
Fig. S9 The AM1.5G solar energy power density and theoretically predicted corrected solar-to-hydrogen efficiency (η_{STH}) with the function of pH at 100% quantum efficiency.

Table S5. Calculated the Over-Potential for HER $\chi(H_2)$, Over-Potential for OER $\chi(O_2)$, and E is the energy of photons of β -PdSe$_2$ monolayer with the function of pH. The energy conversion efficiency of light absorption (η_{abs}), carrier utilization (η_{cu}), STH (η_{STH}) and corrected STH (η'_{STH}).

pH	$\chi(H_2)$ (eV)	$\chi(O_2)$ (eV)	E (eV)	η_{abs} (%)	η_{cu} (%)	η_{STH} (%)	η'_{STH}(%)
0	0.71	0.02	2.54	38.29	18.40	7.04	5.00
1	0.65	0.08	2.48	38.29	20.65	7.90	5.62
2	0.59	0.14	2.42	38.29	23.08	8.83	6.27
3	0.53	0.20	2.36	38.29	25.68	9.83	7.00
4	0.47	0.26	2.30	38.29	28.64	10.96	7.78
5	0.41	0.31	2.24	38.29	31.88	12.20	8.66
6	0.35	0.37	2.19	38.29	34.51	13.21	9.38

7	0.29	0.43	2.13	38.29	38.04	14.56	10.34
8	0.23	0.50	2.07	38.29	41.84	16.02	11.37
9	0.18	0.55	2.03	38.29	44.60	17.07	12.12
10	0.12	0.61	2.04	38.29	43.91	16.81	11.94
11	0.06	0.67	2.10	38.29	40.0	15.31	10.87
12	0.003	0.73	2.15	38.29	36.93	14.14	10.04

References

1. J. Sun, H. Shi, T. Siegrist and D. J. Singh, *Applied Physics Letters*, 2015, **107**, 153902.

2. Z. Wu, L. Lu, X. Liang, C. Dun, S. Yan, E. Mu, Y. Liu and Z. Hu, *The Journal of Physical Chemistry C*, 2020, **124**, 10935-10940.

3. Y. Zuo, Y. Liu, J. Li, R. Du, X. Han, T. Zhang, J. Arbiol, N. r. J. Divins, J. Llorca and N. s. Guijarro, *Chemistry of materials*, 2019, **31**, 7732-7743.

4. Bagger A.; Castelli I E.; Hansen M H.; Rossmeisl J., *Berlin: Springer* **2018,** pp 1–31.

5. R. Kumar, D. Das and A. K. Singh, *Journal of Catalysis*, 2018, **359**, 143-150.

6. Q. Tang and D.-e. Jiang, *Acs Catalysis*, 2016, **6**, 4953-4961.